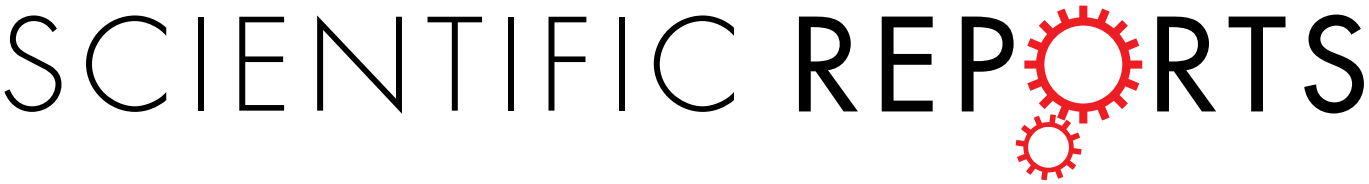

OPEN

# PMCA-replicated $PrP^D$ in urine of vCJD patients maintains infectivity and strain characteristics of brain $PrP^D$: Transmission study

Received: 6 November 2018
Accepted: 14 March 2019
Published online: 26 March 2019

Ignazio Cali[1], Jody Lavrich[1], Fabio Moda[2], Diane Kofskey[1], Satish Kumar Nemani[1], Brian Appleby[3], Fabrizio Tagliavini[2], Claudio Soto[4], Pierluigi Gambetti[1] & Silvio Notari[1]

**The presence of abnormal, disease-related prion protein ($PrP^D$) has recently been demonstrated by protein misfolding cyclic amplification (PMCA) in urine of patients affected with variant Creutzfeldt-Jakob disease (vCJD), a prion disease typically acquired from consumption of prion contaminated bovine meat. The complexity and multistage process of urine excretion along with the obligatory use of PMCA raise the issue of whether strain characteristics of the $PrP^D$ present in vCJD brains, such as infectivity and phenotype determination, are maintained in urine excreted $PrP^D$ and following amplification by PMCA. We inoculated transgenic mice expressing normal human PrP with amplified urine and brain homogenate achieving the same 100% attack rate, similar incubation periods (in both cases extremely long) and histopathological features as for type and severity of the lesions. Furthermore, $PrP^D$ characteristics analyzed by immunoblot and conformational stability immunoassay were indistinguishable. Inoculation of raw vCJD urine caused no disease, confirming the extremely low concentration of $PrP^D$ in vCJD urine. These findings show that strain characteristics of vCJD brain $PrP^D$, including infectivity, are preserved in $PrP^D$ present in urine and are faithfully amplified by means of PMCA; moreover, they suggest that the $PrP^D$ urine test might allow for the diagnosis and identification of disease subtype also in sporadic CJD.**

The diversity of human prion diseases is in part due to the presence of three etiological forms — sporadic, inherited and acquired by infection — while in all other neurodegenerative diseases only the sporadic and inherited forms are currently recognized[1,2]. Furthermore, available evidence points to the brain as the organ where prion diseases start in the sporadic and most inherited forms[2]. By contrast, the great majority of acquired human prion diseases including iatrogenic and variant (v) Creutzfeldt-Jakob disease (CJD), start in peripheral tissues and subsequently propagate to the central nervous system[3]. vCJD, a condition characteristically acquired by consumption of prion contaminated bovine meat[4,5], is a case in point. In vCJD, conversion by the bovine prion of the host normal or cellular prion protein ($PrP^C$) generating a human abnormal and disease-related PrP ($PrP^D$) appears to occur in the gut-associated lymphoid tissues and to propagate to the brain following route(s) yet to be completely defined[6–8]. Many visceral organs and peripheral body fluids such as blood and urine may be exposed to prion infection during this process[3]. Indeed, in vCJD, the presence of proteinase K (PK)-resistant $PrP^D$ ($resPrP^D$) has been shown in several visceral organs, including adrenal gland, spleen, mesenteric lymph nodes, liver, pancreas and kidney[9,10]. Recently, we have demonstrated the presence of minute amounts of $PrP^D$ in urine of vCJD patients[11]. Using protein misfolding cyclic amplification (PMCA), $PrP^D$ was reliably detected affording an accurate and non-invasive diagnostic test of prion disease[11]. By contrast, demonstration of $PrP^D$ in urine of patients with sCJD has been more challenging[11,12].

[1]Case Western Reserve University, Department of Pathology, Cleveland, Ohio, USA. [2]Fondazione IRCCS Istituto Neurologico Carlo Besta, Neurology 5 and Neuropathology Unit, Milano, Italy. [3]Case Western Reserve University, National Prion Disease Pathology Surveillance Center and Departments of Neurology and Psychiatry, Cleveland, Ohio, USA. [4]University of Texas Health Science Center, Department of Neurology, Houston, Texas, USA. Correspondence and requests for materials should be addressed to P.G. (email: pxg13@case.edu) or S.N. (email: sxn194@case.edu)

| Inoculum | Histology & immunohist. | | resPrP$^{D}$ Western blot | | |
|---|---|---|---|---|---|
| | Attack rate (posit./tot.) | Incubation periods (dpi)[c] | Attack rate (posit./tot.) | PrP$^{D}$ type | Incubation periods (dpi)[c] |
| PMCA-treated vCJD urine[a] (1x)[b] | 5/5 | 679 ± 39 | 9/9 | T2B[d] | 661 ± 45 |
| PMCA-treated vCJD urine (1:10)[b] | 3/3 | 718 ± 21 | 8/8 | T2B | 713 ± 36* |
| PMCA of unseeded substrate | 0/4 | 0/718 ± 18 | 0/9 | — | 0/673 ± 182 |
| Raw vCJD urine | 0/52 | 0/700 ± 179 | 0/96 | — | 0/707 ± 148 |
| vCJD BH 10% | 6/6 | 615 ± 78 | 9/9 | T2B | 574 ± 104* |
| vCJD BH 1% | 2/2 | 657 ± 51 | 3/3 | T2B | 648 ± 39 |

**Table 1.** Transmission to Tg40 mice of PMCA-treated vCJD urine, PMCA negative control, untreated vCJD urine and vCJD brain homogenate (BH). [a]Six rounds of PMCA have been performed on the resuspended pellet derived from 1 ml urine. [b]Inoculum 1x and 1:10 correspond to undiluted and to diluted 1:10, respectively. [c]dpi values are express as mean ± standard deviation. [d]T2B means type 2B and identifies the typical electrophoretic profile of vCJD resPrP$^{D}$. *Statistically significant difference ($p < 0.002$) between adjacent T2B values.

The mechanisms leading to the presence of PrP$^{D}$ in urine of vCJD patients remain to be determined[11,12]. The complex, multistage process of urine formation, raises the possibility that, while spreading to urine, PrP$^{D}$ undergo subtle conformational changes altering strain characteristics. Moreover, this issue is further compounded by the extreme under-representation of PrP$^{D}$ in urine that requires extensive amplification or enrichment procedures[11,12].

Transmission to appropriate hosts has been shown to be a suitable approach to define and compare prion strain properties[13]. To this aim, we inoculated transgenic (Tg) mice expressing human PrP 129 M (Tg40) with PrP$^{D}$ obtained from vCJD urine following PMCA and untreated vCJD brain homogenate (BH). Raw vCJD urine was injected as control. Mice injected with PMCA-treated products and those injected with untreated vCJD BH developed prion diseases that were phenotypically indistinguishable and were characterized by similar attack rates and extended incubation periods. Moreover, resPrP$^{D}$ displayed similar conformational features. By contrast, none of the animals inoculated with untreated vCJD urine developed a prion disease.

These data have been partially presented at Prion 2018 (May 22–25, 2018; Santiago de Compostela, Spain).

## Results

**Transmission characteristics.** Inoculation of Tg40 mice with PMCA-treated vCJD urine resulted in prion disease with an attack rate of 100% and incubation periods, as measured by days post inoculation (dpi), of 661 ± 45 and 713 ± 36, depending on the final dilution (1x or 1:10, respectively) of the inoculated PMCA product (Table 1). These results were comparable to those obtained with the transmission of vCJD BH where attack rate again was always 100% and incubation periods varied between 574 ± 104 and 648 ± 39 dpi, according to the 10% or 1% BH concentration of the inoculum (Table 1). The only statistically significant difference was observed when comparing dpi following inoculation of the more diluted PMCA-treated urine (1:10) to the dpi of the more concentrated vCJD BH (10%) inoculum (Table 1). Inoculation of PMCA-treated unseeded-substrate, as negative control, does not have any effect on mice life span. None of the 96 Tg40 mice inoculated with raw vCJD urine tested positive for prion disease up to 707 dpi.

**Histopathology and immunohistochemistry.** The histopathological features of the Tg40 mice challenged with PMCA-treated urine essentially reproduced type and distribution of the lesions associated with the inoculation of vCJD BH. In both conditions, spongiform degeneration (SD) consisted mostly of large vacuoles that predominantly affected subcortical formations including thalamus, hypothalamus, basal ganglia and brain stem (Figs 1i, iii, row l, and 2A). By contrast, florid plaques (FP) populated mostly the cerebral cortex and, to a lesser extent, subcortical regions and cerebellum (Fig. 1i, iii, rows 2 and 4). Non-FP plaques of various sizes were also seen often lined up along the remnants of the lateral ventricles above the hippocampus (Fig. 1i, iii, row 3).

Diffuse PrP immunostaining codistributed with the SD, with intensities that appeared to match the SD severity (Fig. 1ii, iv, row 1). FP and non-FP were strongly immunostained while stellate apparently pericellular PrP deposits were occasionally seen in the cerebral cortex (Fig. 1ii, iv, rows 2 and 3). PrP immunostaining affected also the cerebellum, including the molecular layer and, occasionally, the granular layer and the deep white matter (Fig. 1ii, iv, row 4).

Lesion profiles showed an overall similar distribution of lesions in Tg mice inoculated with PMCA-treated urine or vCJD BH. However, lesions were slightly more severe in mice challenged with 1x PMCA-treated urine than in those receiving vCJD BH (1% or 10%) or 1:10 diluted PMCA-treated urine (Fig. 2A). Neither prion-related lesions nor PrP$^{D}$ deposits were observed in Tg40 mice inoculated with PMCA-unseeded substrate and raw vCJD urine up to 673 dpi and 707 dpi, respectively (Fig. 2A and data not shown). Morphometric analysis of the density and size of FP in the cerebral cortex revealed no significant differences between the two groups of inoculated mice (Fig. 2B,C).

**PrP$^{D}$ characterization.** Regardless of the inoculum, Tg40 animals injected with PMCA-amplified vCJD urine or with untreated vCJD brain homogenate showed the presence of a PK-resistant PrP$^{D}$ (resPrP$^{D}$) displaying the same electrophoretic profile, which was characterized by the prevalence of the diglycosylated band and the mobility to 19 kDa of the unglycosylated isoform (type 2B) (Fig. 3). resPrP$^{D}$ representation in undiluted

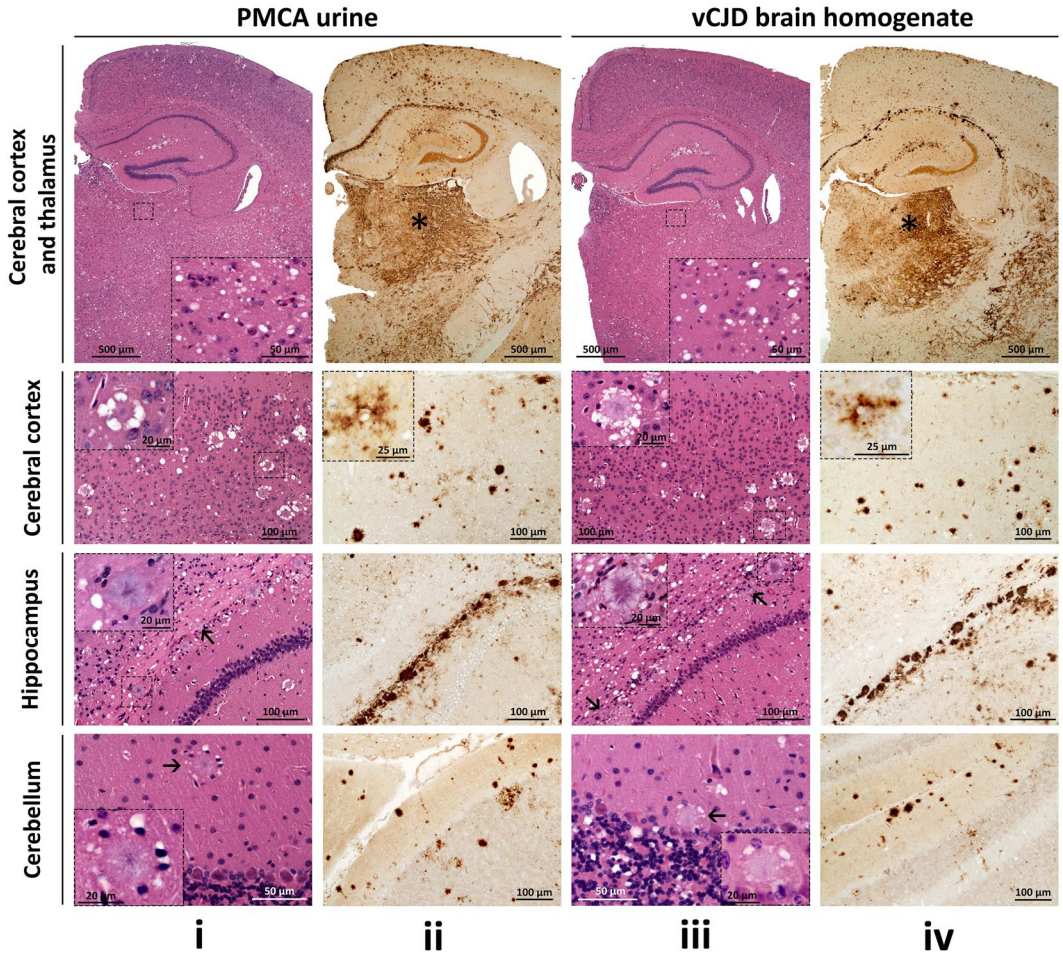


**Figure 1.** Histopathology and PrP immunohistochemistry of brain regions from Tg40 mice. Hematoxylin and eosin (H.E.) staining (i and iii) and PrP immunohistochemistry (ii and iv). i and iii, 1st row: Prominent spongiform degeneration (SD) in subcortical regions. Insets: SD of the thalamus. 2nd row: Typical florid plaques characterized by a dense eosinophilic core and a ring of surrounding SD vacuoles. Insets: individual florid plaques. 3rd row: Non-florid plaques of different sizes at the border between the alveus of the hippocampus and the corpus callosum. Arrows: small plaques. Insets: Non-florid plaques. 4th row: Florid plaques (arrow) populated the molecular layer of the cerebellum. Insets: florid plaques. ii and iv, 1st row: PrP immunostaining of cortical and subcortical regions. PrP immunostaining is particularly intense in the thalamus (asterisk). 2nd row: Intense PrP immunostaining of the florid plaques. Insets: peri-cellular PrP immunostaining ("stellate cells"). 3rd row: Non-florid PrP plaques and loose PrP aggregates distributed along the border between the hippocampal alveus and the corpus callosum. 4th row: PrP plaques and plaque-like PrP aggregates located in the molecular and granular layers of the cerebellum. PrP monoclonal antibody 3F4.

PMCA-treated urine was approximately 20 times lower than that of vCJD BH (10%) (Fig. 3). No $resPrP^D$ was detected in Tg40 mice inoculated with raw vCJD urine (Fig. 3).

The stability of $resPrP^D$ species extracted from Tg40 mice inoculated with either PMCA-treated vCJD urine or vCJD BH was tested with the conformational stability immunoassay (CSI). No significant difference was detected between the two $resPrP^D$ species in their rate of denaturation following treatment with increasing amounts of the denaturant guanidine hydrochloride (GdnHCl). When the GdnHCl treatment was expressed as GdnHCl molar quantity reducing the amount of $resPrP^D$ to half ($[GdnHCl]_{1/2}$), the values obtained were $1.31 \pm 0.1$ M and $1.4 \pm 0.1$ M (Fig. 4).

## Discussion

We have recently shown that urine of patients affected by vCJD harbors minute amounts of $PrP^D$ estimated at $1 \times 10^{-16}$ g/mL, which is approximately 12 orders of magnitude smaller than the $PrP^D$ amount in the vCJD brain tissue ($1 \times 10^{-4}$ g/g)[11]. Despite the small amount, urine $PrP^D$ can be used to diagnose the presence of prion disease in vCJD with 93% sensitivity and 100% specificity[11]. This low $PrP^D$ content is consistent with our finding that none of the 96 Tg40 mice inoculated with raw urine formed detectable $resPrP^D$ especially considering that at least in sCJD the Tg40 limit detectability of brain $PrP^D$ is approximately $1 \times 10^{-5}$ equivalent concentration[14].

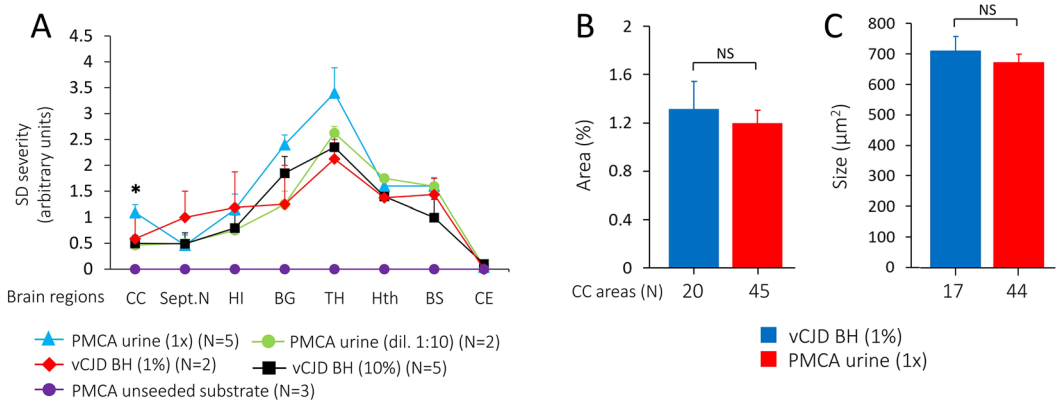


**Figure 2.** Lesion profiles and density of florid plaques in brains of Tg40 mice inoculated with PMCA-treated urine or brain homogenate (BH) from vCJD. (**A**) The profiles of topographic distribution and severity of SD in each group of mice were similar; subcortical regions were predominantly affected with the thalamus showing the most severe lesions. Inoculation of undiluted (1x) PMCA-treated urine resulted in widespread increase of SD which was significantly more severe in the cerebral cortex when compared with the SD in mice inoculated with 10% BH (*$p < 0.03$). No lesions were detected in mice inoculated with PMCA-unseeded substrate. CC: Cerebral cortex; Sept.N: Septal nuclei; HI: Hippocampus; BG: Basal ganglia; TH: Thalamus; Hth: Hypothalamus; BS: Brainstem; CE: Cerebellum. (**B**) Florid plaque burden, expressed as the percentage of the area occupied by the florid plaques, was comparable in the two groups of mice. (**C**) Florid plaque size, expressed in µm². In **B** and **C** values were obtained from the examination of all available CC areas. Similar values were obtained when equal number of areas were compared in the two groups (data not shown). All data are expressed as mean ± SEM. NS: not significant.

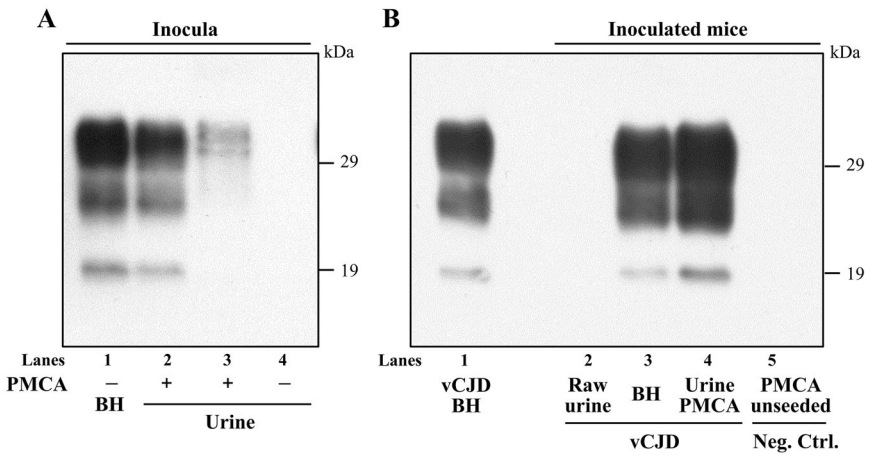


**Figure 3.** Immunoblots of PK-resistant $PrP^D$ ($resPrP^D$) from Tg40 mice inoculated with PMCA-treated vCJD urine and vCJD BH along with native inocula and negative controls. All detected $resPrP^D$ species examined showed the typical T2B profile characterized by the 19 kDa unglycosylated band identifying $resPrP^D$ type 2, and the overrepresentation of the diglycosylated form. (**A**) $resPrP^D$ was detectable in PMCA-treated urine but not in raw urine. Undiluted PMCA-treated urine were loaded 20 or 2 times more than vCJD BH 10% in lanes 2 and 3, respectively. In lane 4 is PMCA-untreated and concentrated urine (1 ml equivalent) after PK digestion. (**B**) No $resPrP^D$ was detected in Tg mice inoculated with raw (non-PMCA-treated) or with unseeded PMCA substrate. BH from Tg40 inoculated with 10% vCJD BH or undiluted PMCA-treated urine (lanes 3 and 4) were loaded 10 times more than vCJD BH 10% (lane 1). Neg. Ctrl.: negative control; inoc.: inoculum. Ab: 3F4.

The complex physiology of urine formation raises the question of how and at which stage $PrP^D$ spreads to urine. Although the precise mechanism remains unidentified, three propagation processes have recently been considered[12]. Given its significant presence in vCJD blood, $PrP^D$ may invade urine during the stage of glomerular filtration, tubular secretion or both. Indeed, increase $PrP^D$ representation in urine has been observed experimentally in the presence of kidney inflammatory processes associated with increase of urine protein excretion[15]. Urine contains relatively high amounts of PrP that is truncated at the N-terminus and harbors an incomplete glycosylphosphatidylinositol anchor suggesting that it is shed from cell surfaces[16]. However, this truncated PrP has been identified as C-terminal fragment C1[16], a product of normal $PrP^C$ metabolism that is an unlikely substrate for conversion to $PrP^D$ since the N-terminal cleavage breaks the 100–130 residue domain considered important

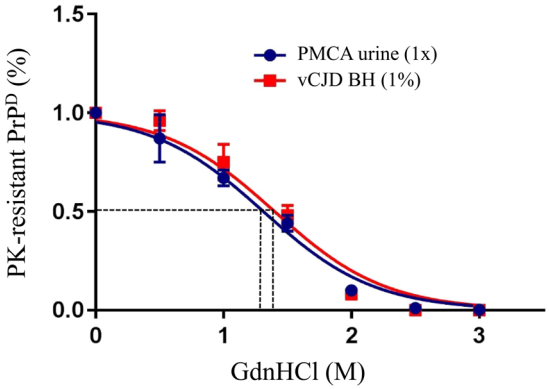


**Figure 4.** Conformational stability immunoassay of resPrP$^D$ from brain of Tg40 inoculated with undiluted PMCA-treated vCJD urine or 1% vCJD BH revealed no statistically significant difference between curves depicting the rate of conversion of resPrP$^D$ to PK-sensitive PrP as a function of the amount of GdnHCl. The guanidine concentrations needed to render half of the PrP$^D$ sensitive to PK, $[GdnHCl]_{1/2}$, were $1.31 \pm 0.1$ M and $1.4 \pm 0.1$ M, respectively (N = 3 for each group).

for the conversion of PrP$^C$ to PrP$^D$[17–21]. It is also noteworthy in this context that contrary to many visceral organs, no PrP$^D$ has been demonstrated in the bladder[9]. Finally, urine PrP$^D$ might result from traditional contiguous PrP$^D$ propagation to urine from kidney, blood or both especially at the level of the nephrons[9,10,12].

In the present study, we show that PMCA-treated urine PrP$^D$ is competent to transmit to Tg mice expressing human PrP a prion disease that, as to the histopathological phenotype and resPrP$^D$ properties, is indistinguishable from the disease transmitted by inoculation with vCJD BH. These findings suggest that urine resPrP$^D$ preserves the strain characteristics of the brain resPrP$^D$. Therefore, the mechanism of urine invasion by PrP, whatever that might be, as well as the PMCA procedure, must preserve the conformational characteristics of brain-generated resPrP$^D$ in vCJD. The present study also confirms the competence of PMCA to accurately replicate PrP$^D$ strain features enciphered in the original seed. This PMCA property, originally reported for the 263K hamster scrapie agent[22–24], is here demonstrated for the first time in a human prion strain. An additional corollary to the present finding is that the non-invasive PMCA-based urine diagnostic test may be used reliably to determine not only the presence of prion disease but also to establish the diagnosis of vCJD.

Presence of PrP$^D$ in urine has been reported in 40% of patients affected with various subtypes of sCJD, by far the most prevalent type of human prion diseases[1], using a solid-state binding matrix to capture and concentrate urine PrP$^D$[12]. By contrast, no PrP$^D$ signal was detected in sCJD urine following the same experimental conditions as those used for PMCA analysis of vCJD urine samples[11]. It has been reported that PrP$^D$ associated with sCJDMM1, the most common subtype of sCJD, is a very inefficient seed for PMCA when using the same conditions described in this article (Camacho *et al*., Prion 2017; May 23–26, 2017; Edinburgh, UK). Finding a solution to this technical hurdle may afford a urine-based diagnostic test that, along with codon 129 PrP genotype determination, may provide the diagnosis of sCJD subtype.

## Materials and Methods

**Biological Safety.** Prion material was handled in a biosafety level 2 (BSL-2) laboratory and all mice were housed in a BSL-2 room of Case Western Reserve University animal facility.

**Urine samples.** Urine samples were obtained from the National Prion Disease Pathology Surveillance Center (NPDPSC). Samples were collected, during the symptomatic period, from a vCJD patient, who died at 25 years of age, 32 months after clinical onset[9,25]. Urine samples were stored at −80 °C until use.

**Protein misfolding cyclic amplification (PMCA).** PMCA of vCJD urine and unseeded substrate was carried out as previously reported[11]. Briefly, 1 ml of urine was centrifuged at low speed (5000 × *g* for 20 minutes at 4 °C) to separate debris. Two fractions, supernatant (S1) and pellet (P1), were obtained. S1 was then centrifuged at high speed (100,000 × *g* for 1 hour at 4 °C) and the pellet (P2a) directly resuspended in 10% homogenate (BH) prepared from brains of transgenic (Tg) mice expressing human PrP-129M (Tg line with PMCA efficiency higher than that of Tg40), which also served as substrate for PMCA. P1, containing cellular debris, was resuspended in 1 ml of water and subjected to high-speed centrifugation (100,000 × *g* for 1 hour at 4 °C). The pellet (P2b) was resuspended in Tg mice-BH, and identified as P2a. The two resuspended pellets (P2a and P2b) were pooled and processed through PMCA cycles. After 96 cycles, the Tg mouse PrP$^C$ substrate was refreshed, and sample subjected to a new round of PMCA cycles. The final sample was obtained after 6 rounds of PMCA. The same Tg mouse BH used as a substrate, left unseeded and similarly treated with 6 rounds of PMCA served as negative control.

**Transgenic mice and inoculations.** Tg mice expressing wild type level human PrP-129M in mouse PrP null background (Tg40), were used for the transmission study[26]. One hundred thirty four Tg40 mice received

intracerebral inoculation (30 µl) of the following samples: (i) PMCA-treated vCJD urine undiluted (1x) or diluted 1:10 (9 and 8 mice, respectively); (iii) vCJD-BH from the same urine donor at 10% or 1% w/v concentration (9 and 3 mice, respectively); (iii) substrate subjected to PMCA without being supplemented with vCJD-urine samples as negative control (9 mice), and (iv) raw vCJD urine (96 mice).

**Histopathology, immunohistochemistry, lesion profiles and morphometric analysis.** Mouse brains were harvested and bisected along the inter-hemispheric fissure. One half was stored at −80 °C until needed for biochemical studies; the other was fixed in formalin and used for histopathological and immunohistochemical examinations. Four coronal slices, obtained from the formalin-fixed half brain, at approximately bregma 0.5 mm, −1.7 mm, −3.8 mm and −6.0 mm, were processed for microscopic examination following staining with hematoxylin and eosin (H.E.) or immunostaining with monoclonal antibody (mAb) 3F4 as previously described[27,28].

Lesion profiles were generated by semi-quantitative evaluation of the severity of spongiform degeneration (SD) on a 0–4 scale, in eight brain regions examined on H&E stained sections (also see Fig. 1). Morphometric analysis to assess density of florid plaques was performed as previously described[29]. Briefly, morphometric analysis was carried out on dorsal, intermediate and ventral cerebral cortices at the three anterior bregma levels. Density was expressed as percentage of the cortical area occupied by florid plaques, whereas size was expressed in $\mu m^2$, and calculated by dividing the area occupied by the florid plaques for their number. To obtain a comparable sample size, the random function (Excel software) was used to randomly select areas of cerebral cortex.

**Western blot.** Ten percent BH, (10% w/v) were prepared on ice in PBS Sarkosyl 2% and aliquots digested with 20U/ml PK (corresponding to 400 µg/ml when PK specific activity is 50U/mg) (Roche Diagnostics) for 1 h at 37 °C. 1 ml of PMCA-untreated vCJD-urine was centrifuged at high speed (100,000 × *g* for 1 hour at 4 °C) and PK digestion (5U/ml, corresponding to 100 µg/ml when PK specific activity is 50U/mg), was performed for 1 h at 37 °C on the pellet resuspended in 10 µl of PBS Sarkosyl 2%. PK digested. The PK digested samples were diluted in sample buffer (final concentration: 3% SDS, 4% β-mercaptoethanol, 10% glycerol, 2 mM EDTA, 62.5 mM Tris, pH 6.8) and boiled for 8 min before loading. Protein samples were separated with Tris-Glycine SDS-PAGE in 15% Criterion Tris-HCl polyacrylamide precast gels (Bio-Rad Laboratories, Hercules, CA, USA) and transferred to Immobilon-P PVDF transfer membrane (EMD-Millipore, Billerica, MA, USA) for 2 h at 60 V, blocked with 5% nonfat dry milk in 0.1% Tween 20-Tris-buffered saline, pH 7.5, and probed with the monoclonal anti-PrP antibody 3F4[27]. The immunoreactivity was visualized by enhanced chemiluminescence (Pierce ECL 2, Fisher Scientific, Hampton, NH, USA) on Kodak BioMax Light films (Eastman Kodak Co., Rochester, NY, USA).

**Conformational stability immunoassay (CSI).** CSI was performed as previously described[30–32] with minor modifications. Aliquots of 10% BH in LB100 pH 8.0 (100 mM Tris HCl pH 8.0, 100 mM NaCl, 0.5% Nonidet P-40, 0.5% sodium deoxycholate, 10 mM EDTA) were centrifuged for 10 min at 1,000 × g at 4 °C and pellets discarded. 100 µl of the supernatants were diluted with an equal volume of GdnHCl to obtain a final concentration ranging from 0 to 4 M and incubated for 1.5 h at room temperature. GdnHCl was subsequently removed by precipitation with 5 volumes of methanol with overnight incubation at −20 °C and centrifuged for 30 min at 18,000 × g. Pellets were resuspended in 100 µl LB 100 pH 8.0 by sonication. Each aliquot was digested with 5U/ml PK for 1 h at 37 °C. The reaction was stopped by addition of 2 mM PMSF. After denaturation, samples were analyzed by WB (Ab: 3F4) and developed by Odyssey Classic infrared imaging system (LI-COR Biosciences). PrP densitometry was performed by Odyssey V3.0 software (LI-COR Biosciences). After normalization, the data were plotted and expressed as mean ± standard deviation. Conformational stability, evaluated as a function of $resPrP^D$ conversion to PK-sensitive PrP following exposure to increasing concentrations of GdnHCl, was best fitted to a sigmoidal dose-response equation by GraphPad Prism 7 (GraphPad Software Inc.). The formula $[GdnHCl]_{1/2} \pm SD$ was calculated for the two groups and compared by statistical analysis.

**Statistical analysis.** Statistical analyses were performed with (i) Student's T-test, for lesion profile, florid plaque density-size analyses, and conformational stability immunoassay, and (ii) analysis of variance (One-Way ANOVA) followed by Tukey's multiple comparison test, for incubation periods (days post inoculation, dpi).

**Ethics statement.** The human samples used in the current study were provided by NPDPSC. Written informed consent for research was obtained from the patient according to the Declaration of Helsinki. No minor participants were included in the study. All procedures were performed under protocols approved by the Institutional Review Board for Human Investigation of University Hospitals, Case Medical Center of Cleveland, OH, and as per regulations of the Declaration of Helsinki. All animal studies were carried out in accordance with the recommendations in the Guide for the Care and Use of Laboratory Animals of the National Institutes of Health. The protocols were approved by the Institutional Animal Care and Use Committee of the Case Western Reserve University (Protocol number 2012-0199).

## Data Availability

All data generated or analysed during this study are included in this published article.

## References

1. Gambetti, P. *et al*. Molecular biology and pathology of prion strains in sporadic human prion diseases. *Acta Neuropathol* **121**, 79–90 (2011).
2. Ritchie, D. L. & Ironside, J. W. Neuropathology of Human Prion Diseases. *Prog Mol Biol Transl Sci* **150**, 319–339 (2017).

3. Head, M. W. *et al*. Peripheral tissue involvement in sporadic, iatrogenic, and variant Creutzfeldt-Jakob disease: an immunohistochemical, quantitative, and biochemical study. *Am J Pathol* **164**, 143–153 (2004).
4. Bruce, M. E. *et al*. Transmissions to mice indicate that 'new variant' CJD is caused by the BSE agent. *Nature* **389**, 498–501 (1997).
5. Hill, A. F. *et al*. The same prion strain causes vCJD and BSE. *Nature* **389**, 448–450 (1997).
6. Aguzzi, A., Nuvolone, M. & Zhu, C. The immunobiology of prion diseases. *Nat Rev Immunol* **13**, 888–902 (2013).
7. Donaldson, D. S., Else, K. J. & Mabbott, N. A. The Gut-Associated Lymphoid Tissues in the Small Intestine, Not the Large Intestine, Play a Major Role in Oral Prion Disease Pathogenesis. *J Virol* **89**, 9532–9547 (2015).
8. Mabbott, N. A. How do $PrP^{Sc}$ Prions Spread between Host Species, and within Hosts? Pathogens **6**(4) (2017).
9. Notari, S. *et al*. Multiorgan detection and characterization of protease-resistant prion protein in a case of variant CJD examined in the United States. *PLoS One* **5**(1), e8765 (2010).
10. Douet, J. Y. *et al*. Distribution and Quantitative Estimates of Variant Creutzfeldt-Jakob Disease Prions in Tissues of Clinical and Asymptomatic Patients. *Emerg Infect Dis* **23**, 946–956 (2017).
11. Moda, F. *et al*. Prions in the urine of patients with variant Creutzfeldt-Jakob disease. *N Engl J Med* **371**, 530–539 (2014).
12. Luk, C. *et al*. Diagnosing Sporadic Creutzfeldt-Jakob Disease by the Detection of Abnormal Prion Protein in Patient Urine. *JAMA Neurol* **73**, 1454–1460 (2016).
13. Boyle, A., Hogan, K., Manson, J. C. & Diack, A. B. Strain Typing of Prion Diseases Using *In Vivo* Mouse Models. *Methods Mol Biol* **1658**, 263–283 (2017).
14. Notari, S. *et al*. Assessing prion infectivity of human urine in sporadic Creutzfeldt-Jakob disease. *Emerg Infect Dis* **18**, 21–28 (2012).
15. Seeger, H. *et al*. Coincident scrapie infection and nephritis lead to urinary prion excretion. *Science* **310**, 324–326 (2005).
16. Dagdanova, A. *et al*. Characterization of the prion protein in human urine. *J Biol Chem* **285**, 30489–30495 (2010).
17. Gasset, M. *et al*. Predicted alpha-helical regions of the prion protein when synthesized as peptides form amyloid. *Proc Natl Acad Sci USA* **89**, 10940–10944 (1992).
18. Tagliavini, F. *et al*. Synthetic peptides homologous to prion protein residues 106–147 form amyloid-like fibrils *in vitro*. *Proc Natl Acad Sci USA* **90**, 9678–9682 (1993).
19. Chen, S. G. *et al*. Truncated forms of the human prion protein in normal brain and in prion diseases. *J Biol Chem* **270**, 19173–19180 (1995).
20. Muramoto, T., Scott, M., Cohen, F. E. & Prusiner, S. B. Recombinant scrapie-like prion protein of 106 amino acids is soluble. *Proc Natl Acad Sci USA* **93**, 15457–15462 (1996).
21. Solforosi, L. *et al*. Toward molecular dissection of $PrP^{C}$-$PrP^{Sc}$ interactions. *J Biol Chem* **282**, 7465–7471 (2007).
22. Castilla, J., Saá, P., Hetz, C. & Soto, C. *In vitro* generation of infectious scrapie prions. *Cell* **121**, 195–206 (2005).
23. Meade-White, K. D. *et al*. Characteristics of 263K scrapie agent in multiple hamster species. *Emerg Infect Dis* **15**, 207–215 (2009).
24. Gonzalez-Romero, D., Barria, M. A., Leon, P., Morales, R. & Soto, C. Detection of infectious prions in urine. *FEBS Lett* **582**, 3161–3166 (2008).
25. Belay, E. D. *et al*. Variant Creutzfeldt-Jakob disease death, United States. *Emerg Infect Dis* **11**, 1351–1354 (2005).
26. Kong, Q. *et al*. Chronic wasting disease of elk: transmissibility to humans examined by transgenic mouse models. *J Neurosci* **25**, 7944–7949 (2005).
27. Kascsak, R. J. *et al*. Mouse polyclonal and monoclonal antibody to scrapie-associated fibril proteins. *J Virol* **61**, 3688–3693 (1987).
28. Notari, S. *et al*. Transmission characteristics of variably protease-sensitive prionopathy. *Emerg Infect Dis* **20**, 2006–2014 (2014).
29. Cali, I. *et al*. Iatrogenic Creutzfeldt-Jakob disease with Amyloid-β pathology: an international study. *Acta Neuropathol Commun* **6**(1), 5 (2018).
30. Zou, W. Q., Zheng, J., Gray, D. M., Gambetti, P. & Chen, S. G. Antibody to DNA detects scrapie but not normal prion protein. *ProcNatl Acad Sci USA* **101**, 1380–1385 (2004).
31. Pastore, M. *et al*. Creutzfeldt-Jakob disease (CJD) with a mutation at codon 148 of prion protein gene: relationship with sporadic CJD. *Am J Pathol* **167**, 1729–1738 (2005).
32. Cali, I. *et al*. Co-existence of scrapie prion protein types 1 and 2 in sporadic Creutzfeldt-Jakob disease: its effect on the phenotype and prion-type characteristics. *Brain* **132**, 2643–2658 (2009).


## Acknowledgements

We thank the patient families, referring clinicians, The CJD Foundation, the NPDPSC technical and administrative personnel, in particular Mss. Janis Blevins, Katie Glisic, Yvonne Cohen, Wei Chen and Miriam Warren for their invaluable assistance. This study was supported in part by NIH grant 5P01AI106705 to PG and CS, NIH 5R01NS083687 and Charles S. Britton Fund to PG.

## Author Contributions

I.C. performed experiments and analyzed the data. J.L., F.M., D.K., S.K.N. performed experiments. BA provided the human tissues necessary to perform the study. F.T. supervised the work. C.S. and P.G. conceived the study. P.G. and S.N. designed the experiments, coordinated the project, analyzed the data and wrote the manuscript. All authors edited the paper. All authors read and approved the final manuscript.

## Additional Information

**Competing Interests:** Dr. Soto is inventor on several patents related to the PMCA technology and is currently Founder, Chief Scientific Officer and Vice-President of Amprion Inc, a biotech company focusing on the commercial utilization of PMCA for prion diagnosis.

**Publisher's note:** Springer Nature remains neutral with regard to jurisdictional claims in published maps and institutional affiliations.